Asian Pub. Corp.

www.asianpubs.org

ARTICLE

Computational, Experimental Structural Characterization and Molecular Docking Studies of 5,7-Dihydroxy-4-methoxyflavone against Cytochrome P450 Enzymes

A. Harikrishnan[1,✉] and R. Madivanane[2]

Asian Journal of Organic & Medicinal Chemistry

Volume: 5 Year: 2020
Issue: 3 Month: July–September
pp: 197–207
DOI: https://doi.org/10.14233/ajomc.2020.AJOMC-P275

Received: 2 May 2020
Accepted: 7 August 2020
Published: 15 September 2020

ABSTRACT

In this work, the geometry optimization and harmonic vibrational wavenumbers of kaempferide (5,7-dihydroxy-4-methoxyflavone) were computed by density functional theory (DFT) method. Theoretically computed vibrational wavenumbers were compared with experimental values and the interpretation of the vibrational spectra has been studied. Frontier molecular orbitals (FMO) and molecular electrostatic potential (MEP) analysis of the title compound have been carried out. The ^{1}H & ^{13}C NMR, UV visible and electronic properties of the compound were investigated theoretically and compared with the experimental values. Molecular docking study of the compound against cytochrome P450 family enzymes (CYPs 1A1, 1A2, 3A4, 2C8, 2C9 and 2D6) were also studied and the results revealed that the title compound interact with human CYP2C8 enzymes with minimum binding energy of -9.43 kcal/mol. The compound forms hydrogen bond with the residues of Thr302, Thr305, Leu361, Val362, Cys435, Gln356 and Ala297. Thus, these studies assist to understand the inhibitory mechanism of kaempferide with CYP450 enzymes and may facilitate significant clinical implications in the prevention and treatment of various therapeutic diseases.

KEYWORDS

Kaempferide, Cytochrome P450, Nucleophilic, Electrophilic, Molecular docking, Binding energy.

INTRODUCTION

Flavonoids are the major polyphenolic compounds present in wide variety of plant products such as fruits, vegetables and beverages [1,2]. Flavonoids posses C_6-C_3-C_6 carbon skeleton, consisting of two phenyl rings A and B connected by a three carbons and an oxygen bridge that forms the heterocyclic pyran ring C (Fig. 1). The chemical nature of flavonoids depends on their various levels substitutions such as hydroxylation, methoxylation, conjugations and other substitutions. Based on the oxidation level of ring C, flavonoids are classified as flavonols, flavones, flavanones, isoflavones, chalcones and anthocyanidins. From the literature review, it can be seen that a wide range of pharmacological properties has been associated with flavonoids such as antioxidant, antibacterial, antifungal, antihepatotoxic, antitumor, anti-HIV-1 [3].

Author affiliations:

[1]Department of Physics, Bharathiar University, Coimbatore-641046, India
[2]Department of Physics, Bharathidasan Government College for Women, Puducherry-605001, India

✉To whom correspondence to be addressed:

E-mail: krish53hari80@gmail.com

Available online at: http://ajomc.asianpubs.org

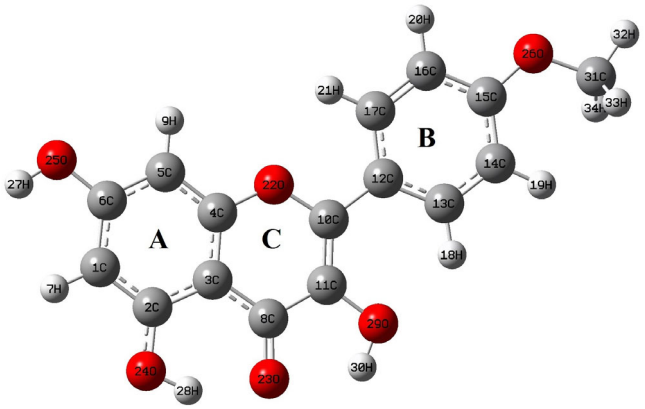

Fig. 1. Ground state optimized structure of kaempferide with atom numbering

Taking into account the wide range of biological properties of flavonoids, especially in the human organism, the study of flavonoids is considered a subject of great interest. In this work, one of the most important flavonoid kaempferide was subjected to combined experimental and theoretical study on molecular and vibrational frequencies based on FTIR, FT-Raman spectra, Hartree-Fock (HF) and density functional theory (DFT) methods.

Kaempferide, a common naturally occuring flavo-noid under the subcategory of flavonol, is isolated from roots of *Alpinia officinarum* [4]. It has broad spectrum importance, researchers have been reporting its various pharmacotherapeutic activities, such as antitrypanosomal and antileishmanial [5], antioxidant [6], antiradical and free radical scavenging activities [7]. Nath *et al.* [8] reported that kaempferide prompts a dose dependent cytotoxicity in cervical tumor cells and incites caspase dependent apoptosis in HeLa cells. Kaempferide showed cys-LTs release inhibitory activity from differentiated HL-60 cells [9] and also showed comparatively strong cytotoxicity toward HT-1080 tumor cells and colon 26-L5 cells [10]. In addition, the *in vitro* and *in vivo* study clearly indicate that kaempferide is non-toxic to ordinary fibroblasts, which could be assessed by acute and chronic toxicity studies in Swiss albino mice [8]. In addition, a quantum chemical and molecular docking study of kaempferide on inhibiting the aggregate formation of mutant SOD1 protein in familial amyotrophic lateral sclerosis was studied by Srinivasan and Rajasekaran [11]. The efficacy mechanism of kaempferide against myocardial ischemia/reperfusion injury through activation of the PI3K/Akt/GSK-3β pathway for the treatment of cardiovascular disease was studied by Wang *et al.* [12]. The antiproliferative activity of kaempferide on human cancer cell lines was studied by Nguyen *et al.* [13]. The pharmacological mechanisms of keampferide in the treatment of vitiligo by the induction of melanogenesis *via* upregulation of melaninbiosynthetic genes, was studied by Wang *et al.* [14]. The inhibitory effect of kaempferide on adipocyte differentiation and their mechanisms involving mitotic clonal expansion (MCE) and apoptosis during the early stage of adipogenesis were investigated by Kumkarnjana *et al.* [15]. The dual effect of kaempferide to induce apoptosis in putative cancer stem cell in myeloma and reverse drug transporter activity were investigated by Loh *et al.* [16]. Recently, DFT calculations combined with FTIR and FT-Raman spectroscopy techniques have been used as important tools to study molecular structure of the biological compounds [17]. According to literature, a combined FTIR and FT-Raman experimental and quantum chemical computations study of flavone were examined by Erdogdu *et al.* [18]. Milenkovic *et al.* [19] discussed molecular structure and vibration frequencies of kaempferol with experimental and theoretical vibrational frequency and interpreted IR and Raman spectra. The DFT calculations on molecular structure, infrared and ultraviolet spectra of the flavonoid compound quercetin were studied by Mendoza-Wilson *et al.* [20]. The FT-IR and FT-Raman vibrational spectroscopic and molecular structural study of apigenin has been carried out by Mariappan *et al.* [21]. The investigation of molecular structure and vibration frequencies of chrysin with FT-IR and FT-Raman spectroscopy and quantum chemical calculations were carried out by Sundaraganesan *et al.* [22]. Cornard *et al.* [23] studied the molecular structural and vibrational study of 3-hydroxyflavone and 3-methoxyflavone by semi empirical calculations AM1 method. From the literature survey, it has been presumed that to the best of our knowledge, no experimental FTIR/FT-Raman and *ab initio* HF/DFT fre-quency calculations of kaempferide have been accounted so far. Due to the remarkable scope of biological activities of kaempferide, we interested to work an experimental FTIR and FT-Raman vibrational spectroscopic and theoretical quantum computational calculations utilizing HF and DFT (B3LYP) methods. In this study, we reported the theoretical calculations on molecular structure and vibrational spectra of kaempferide by interpret with IR and Raman spectra. In addition, nuclear magnetic resonance (NMR), UV-visible electronic properties, highest occupied molecular orbital (HOMO), lowest unoccupied molecular orbital (LUMO) energies and molecular electrostatic potential (MEP) analysis of the compound has also been reported to understand the molecular structure and its various natural movement as per substitution places of hydroxyl or methoxy groups.

Furthermore, molecular docking methodology was used in the present study to analyze the binding mechanism of the compound kaempferide with different CYP enzymes. Cytochromes P450 (CYPs) are hemethiolate monooxygense enzymes mostly expressed in all tissues, such as, small intestinal mucosa, lung, kidney, cerebrum, placenta, olfactory mucosa and skin [24]. CYPs, those shares not less than 40% of the amino acid sequence identity are grouped into family (CYP1, CYP2 CYP3). Besides, if they share more than 55% sequence identity, are grouped into subfamilies (CYP1A1, CYP1A2 and CYP1B1). In human, CYPs 1A1, 1A2, 3A4, 1B1, 2C8, 2C9 and 2D6 are vital catalysts which have an imperative part in the digestion of endogenous, exogenous compound. At present moment, over half of the drug accessible in the business sectors is metabolized by CYPs [25]. The CYPs are related with the metabolic actuation of various cancer causing agents, procarcinogens and chemotherapeutics, which are responsible for metabolizing various therapeutic drugs. An inhibition of CYPs plays a vital role in the treatment of a few disease conditions and particularly for the treatment and prevention of cancer. Studies have shown that the inhibition mechanism of CYP450 by diverse flavonoid derivatives has been widely reported by research community. The inhibition few CYP450s, such as, CYPs 1A1, 1A2, 1B1,

2C9, 3A4 by the flavonoid compounds bringing about prevention of cancer carcinogens [26]. Shimada *et al.* [27] performed molecular docking and quantitative structure activity relationship studies for several flavonoids on the X-ray crystal structure of CYP1A2. The inhibitory effect of the flavonoids: Hesperetin, pinocembrin, acacetin, chrysin, chrysin-dimethylether, flavone, tangeretin, galangin, isorhamnetin, morin and tamarixetin on the CYP1A2, CYP2A6, CYP2C8 and CYP2D6 enzymes were reported by Bojic *et al.* [28]. The inhibition of several flavone propargyl ethers on CYP1A1 and CYP1A2 have been investigated and compared to CYP2A6 and CYP2B1 [29]. Sridhar *et al.* [30] showed that the inhibition activity of 7-hydroxyflavone on CYP1A1 and the QSAR (Quantitative structure-activity relationships) studies of flavone on CYP1A1 enzymes have been performed by Iori *et al.* [31]. The binding mechanism of naringenin to human CYP1A1 has been studied through molecular docking [32]. The binding interaction of flavonoid compounds with CYP P450 enzyme aromatase, which is involved in the metabolism of estrogens for treatment of estrogen-dependent breast cancers were studied by Indu *et al.* [33]. The *in silico* metabolism studies of flavonoids compounds such as quercetin, rutin, naringenin and naringin by CYP1A2 and CYP2C9 were investigated by Sousa *et al.* [34]. The analysis of interaction between methoxyflavonoids and amino acid residues in the human CYP1B1 were demonstrated by Takemura *et al.* [35]. The comparative inhibition studies of the flavonoids on the CYP1A1 and CYP1B1 enzymes were performed by Androutsopoulos *et al.* [36]. The inhibition of mediated drug metabolism CYP2C8 by the flavanoid diosmetin and hesperetin was reported by Quintieri *et al.* [37]. The inhibition of flavonoids, naringin, naringenin and quercetin with CYP3A4dependent drug metabolism were investigated by Fasinu et al. [38]. The inhibitory effect of natural flavonoids wogonin, 7-methoxy-flavanone, oroxylin A, baicalein, baicalin, scutellarein and wogonoside on huamn cytochrome P450 1 A (CYP1 A) were demonstrated by Tu *et al.* [39]. Previous studies have reported the inhibition effect of several flavonoids with various CYP450 enzymes; however, the inhibition mechanisms of kaempferide involved in this enzyme remains to be better elucidated. In light of above mentioned facts and in continuation of our efforts in research, in the present study, the interaction of kaempferide with various CYPs (1A1, 1A2, 3A4, 2C8, 2C9 and 2D6) enzymes was reported through molecular docking study. The accommodation of the compound in the binding pocket was the deciding factor in determining the binding orientations in the active sites of CYPs enzymes. The results of this molecular docking could support the biological activity of the compound at the atomic level. Molecular docking study may facilitate to distinguish active sites and assist know about the inhibitory mechanism of the compound in the prevention and treatment of some therapeutic diseases.

EXPERIMENTAL

The Fourier transform infrared spectrum (FTIR) of the sample was recorded in the frequency range of 4000-600 cm^{-1} at 4 cm^{-1} resolution with no further purification. The FT-Raman spectrum (FT-R) of kaempferide was recorded in the region 4000 and 50 cm^{-1} at the resolution of 2 cm^{-1}. Figs. 2 and 3

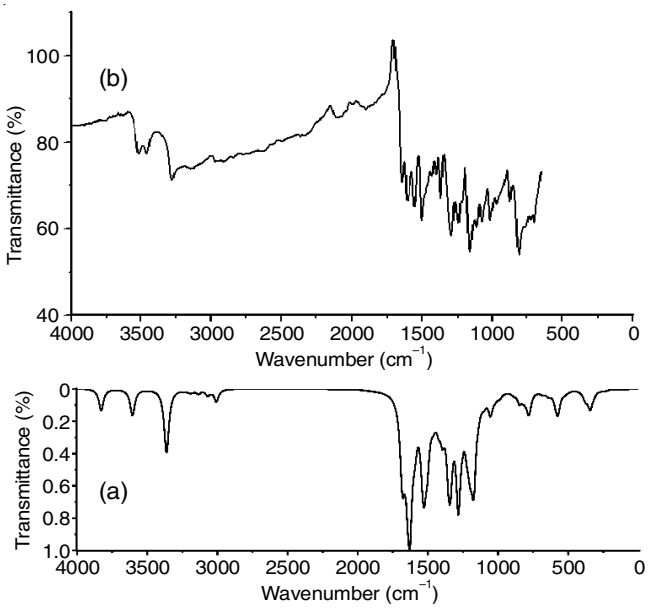

Fig. 2. (a) Simulated (b) experimental FTIR spectrum of kaempferide

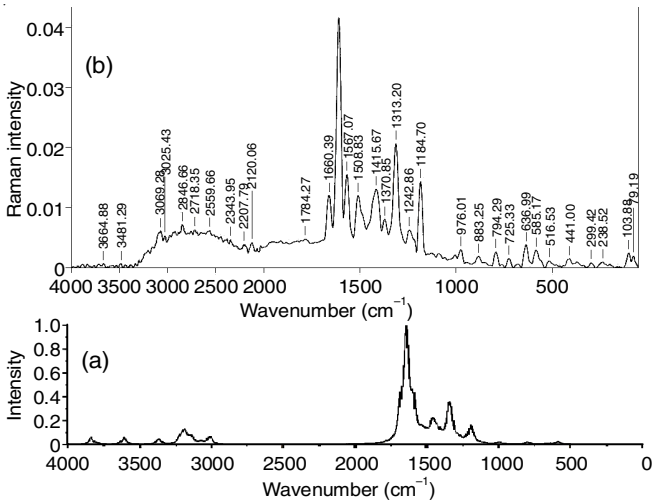

Fig. 3. (a) Simulated (b) experimental FT-Raman spectrum of kaempferide

represents comparison of the simulated and experimental FTIR/FT-Raman spectra of kaempferide, respectively. The complete geometrical optimizations of the kaempferide is performed using the DFT/B3LYP methods with basis set 6-311++G (d,p) implemented in Gaussian 09 program package in a personal computer [40]. Based on the optimized structure (Fig. 1), the frontier molecular orbital (FMOs), molecular electrostatic potentials (MEP) of kaempferide is also computed at a similar level of theory (B3LYP). The ^{1}H & ^{13}C NMR isotropic shielding were computed by the method of GIAO technique at B3LYP/6-31G (d) method. The TD-DFT/B3LYP/6-311++G(d,p) calculations were performed from the fully optimized structure to determine the low-lying excited states of kaempferide. In the present investigation, *in silico* molecular docking studies of kaempferide against human CYPs were performed using Autodock 4.2 with mgltools 1.5.6 [41]. The binding site selection was carried out with grid parameters defined as default, x = 60, y = 60 and z = 60 while the spacing between grid points at 0.375 Å. To find the conformation with the best binding free energy, all rotatable bonds of the ligands were set to be free

whereas the protein molecule was treated as a rigid structure. For each target, ten different docking runs were carried out for a 150 population size with a 2 500 000 maximum number of energy evaluations. Using Lamarckian genetic algorithms docking simulations were performed and the generated results yields RMSD values below 1.95 Å.

RESULTS AND DISCUSSION

Molecular geometry: The mechanisms of antioxidant activity and hydrogen radical donating abilities of the flavanoids have been related with their number of hydroxyl groups in the molecule [42]. The experimentally observed ionization potential calculation demonstrates that the hydroxyl group at C11 and C2 position in the vicinity of C8=O in the flavones, is a significant structural component and causing increased antioxidant activity [43]. Kaempferide molecule comprises of three hydroxyl groups, two of them 24O-28H and 25O-27H are sited in the benzo ring (A) at C2 and C6, the remaining one 29O-30H is to be found in the pyron ring (C) at C11. The optimized geometrical parameters are recorded in Table-1 as per atom numbering. No experimentally observed geometrical parameters available in the literature and hence the calculated structural parameters were compared with those found for similar comparable structure such as quercetin [44], whose values are observed from the X-ray diffraction technique. The theoretically computed bond length and bond angles are somewhat longer than the ones from the experimental data because, the experimental values taken from X-ray diffraction method in solid state, while the theoretical method is the gas phase. The bond length of C8-O23 (1.267 Å) validates the single bond and double bond nature of carbonyl group and hence it is somewhat smaller than the other C-O bond. The X-ray diffraction investigation of 5-hydroxyflavone [45] and quercetin [46,47] exposed that the excited state intramolecular proton transfer (ESIPT) is takes place in between the OH group at C-2 and the carbonyl oxygen (C=O) at C8. In the present study, the excited state intramolecular proton transfer is confirmed by theoretical calculation. A strong intramolecular hydrogen bond is formed between the H28 (O24-H28) and O23 (C=O) with stated distance 1.766 Å. In addition, the DFT method records strong intramolecular H-bond in between the 3-OH (O29) in chromone (C) and hydrogen atom (H18) at 13C of phenyl ring (B) with expressed separation of 2.157 Å. Thus, these two strong H-bonds permit the development of a six membered ring which are coplanar to the chromone part and stabilize the structure. Besides, the possible stable conformity of kaempferide predominantly relies upon the pivot of C10-C12 (1.462 Å). This bond interfaces the phenyl and chromone group and assumes an imperative part in the flexibility and conformational stability of the molecule. Due to the substitution of an electron-accepting hydroxyl group at C2, C6 and C11, there is a deviation of the internal angles to 119.8º, 122.1º and 121.6º, respectively and an elongation in the bond lengths were observed. The C3-C8-C11 bond angle is also reduced to 116.9º due to the substitution of carbonyl group in the chromone (C) ring. Furthermore, the theoretically computed dihedral angle between C11-C10-C12-C13 and C11-C10-C12-C17, C22C10-C12-C17 and C22-C10-C12-C13 are 0º to 180º, respectively. This value is demonstrated in straight agreement with Jin *et al.* [48], who found the dihedral angle 0º to 180º for stable conformation of quercetin molecule.

TABLE-1
SELECTED OPTIMIZED GEOMETRIC PARAMETERS OF KAEMPFERIDE

Bond length (Å)	DFT	Exp. [Ref. 15]	Bond angle (Å)	DFT	Exp. [Ref. 15]
C2-O24	1.341	1.375	C3-C8-C11	116.2	116.9
C4-O22	1.359	1.370	C2-C1-C6	119.6	119.1
C6-O25	1.361	1.358	C1-C2-O24	119.7	119.8
C8-O23	1.257	1.267	C3-C4-O22	120.4	120.1
C10-O22	1.374	1.365	C8-C11-C10	121.6	120.8
C11-O29	1.357	1.351	C11-C10-O22	119.0	120.7
C15-O26	1.359	1.385	C13-C14-C15	120.1	119.9
H18-O29	2.157	–	C14-C15-C16	119.3	120.2
O23-H28	1.766	–	C15-C16-C17	120.4	120.0
O24-H28	0.987	0.948	C12-C17-C16	121.2	120.3
O25-H27	0.963	0.914	C2-O24-H28	107.7	101.9
O29-H30	0.977	0.906	C11-O29-H30	104.5	110.3
C10-C12	1.462	1.479	C6-O25-H27	113.0	110.2

Vibrational spectral analysis: The quantum chemical calculation of kaempferide is computed in vacuum and hence the wave numbers are harmonic ones, while the experiments were performed for solid sample are an anharmonic wave numbers. Consequently, some of the calculated wavenumbers are higher than their experimental esteems and these disparities are rectified by utilizing scaling factor 0.99, 0.98 and 0.97 [49]. The vibrational assignments of kaempferide have been performed based on the animation option of Gauss View 5.0.8 [50] and together with based on potential energy distribution (PED) analysis utilizing VEDA4 program [51]. The calculated (selected) and the corresponding observed wave numbers, vibrational assignments of the title compound are reported in Table-2. These assignments are in good agreement with the literature [49].

NMR analysis: In NMR experiment, nuclear shielding constants are estimated with respect to the reference substance and are given as the chemical shift. For an organic molecule, the ^{13}C NMR chemical shifts are more than 100 ppm and the exactness guarantees interpretation of spectroscopic parameters [52]. In the present investigation, the ^{13}C and ^{1}H magnetic isotropic shielding tensors were ascertained by the GIAO method with inclusion of solvent DMSO using DFT at B3LYP level with basis set 6-31G (d). The isotropic shielding values were used to compute the isotropic chemical shifts with respect to tetramethylsilane (TMS). The calculated chemical shifts values are compared with experimentally observed carbon and proton shifts values and in addition to that it is also compared with the reported literature [8]. The ^{1}H and ^{13}C theoretical and experimental chemical shifts and the assignments of KFD are presented in Table-3. As expected from the literature [53], the ^{13}C NMR chemical shift for the KFD is higher than 100 ppm and an acceptable concurrence is observed in between experimental and theoretical chemical shifts for both carbons and protons. In the ^{13}C NMR, the aromatic carbons C2, C6 and C11 are attached to the hydroxyl groups and resonated at 161.1, 164.4 and 136.5 ppm, respectively. The ^{13}C chemical shifts values of the C11 is marginally more when compared to C2

TABLE-2
EXPERIMENTAL AND CALCULATED VIBRATIONAL FREQUENCIES (cm^{-1}) ASSIGNMENTS OF KAEMPFERIDE

S. No.	Experimental frequencies (cm^{-1})		Calculated frequencies (cm^{-1})		Vibrational assignments (PED %)
	FTIR	FTR	DFT unscaled	DFT scaled	
1	3515	3666	3608	3572	νs OH(100)
2	3461	3481	3366	3332	νs OH(99)
3	3275	3297	3241	3209	νs CH(97)
4	3141		3139	3108	νs CH(91)
5	2916	2972	3011	2981	νs CH(91)
6		1660	1661	1644	νas CC(26) + νas C=O
7	1647		1645	1629	νas CC(30) + νas C=O
8		1609	1602	1586	νs CC(58)+ γ HCC(13)
9	1607		1594	1578	νs CC(38)
10		1567	1542	1527	β HCC(31) + νas CC
11	1508	1508	1507	1492	β HCC(20) + β HCC(10) + νas CC
12	1433		1448	1434	νas CC(13) + γ HCC(17)
13	1402		1399	1385	β HOC(10)
14	1371	1370	1353	1339	β HCC(16) + νas CC(10)
15	1313	1313	1337	1324	β HCC(18) + νas C-O
16	1283		1283	1270	νas CC(21)
17	1250		1258	1245	νs CC(25) + β HCC(10)
18	1165		1167	1155	β HCH(56)
19	1118		1104	1093	νs CC(56)
20	1082	1087	1057	1046	νs OC(70)
21	1019		1022	1012	νas CC(39)
22	973	976	984	974	τ HCCC(79)
23	976	945	967	957	τ HCCC(77) + γ HCC(12)
24	877	848	850	842	τ HCCC(88)
25	809		817	809	τ HCCO(78)
26	766		783	775	τ HCCO(58) + γ HCC(12)
27	702		689	682	γ HCC(14)
28	680	680	683	676	τHCCC(46)
29		636	638	632	τ HCCC(57)
30		585	591	585	γ HCC(36)

νs-symmetric stretching, νas-asymmetric stretching, β-in-plane-bending, γ-out-of-plane bending, τ-torsion. Potential energy distribution (PED); values less than 10% are not shown.

TABLE-3
CALCULATED ^{1}H AND ^{13}C NMR ISOTROPIC CHEMICAL SHIFTS OF KAEMPFERIDE

Atom position	B3LYP/ 6-31G(d)	Exp. [Ref. 2]	Atom position	B3LYP/ 6-31G(d)	Exp. [Ref. 2]
C1	112.4	98.3	H7	6.57	5.95
C2	170.7	163.9	H9	6.56	5.95
C3	111.1	105.5	H18	12.11	7.19
C4	152.6	160.1	H19	8.02	6.72
C5	104.9	98.0	H20	7.04	6.72
C6	171.8	166.4	H21	7.97	7.19
C8	173.3	178.3	H27	4.53	5.0
C10	158.7	160.0	H28	8.98	5.0
C11	149.3	136.6	H30	4.57	15.0
C12	135.8	122.7	H32	3.32	3.73
C13	141.5	127.4	H33	4.33	3.73
C14	122.3	114.2	H34	2.53	3.73
C15	176.7	159.9	–	–	–
C16	122.1	114.2	–	–	–
C17	130.7	127.4	–	–	–
C31	57.7	55.9	–	–	–

and C6, since the hydroxyl groups substituted at C11 influences a hydrogen bond formation. Oxygen atom demonstrates an electronegative property in which the higher ^{13}C chemical shift esteem (176.4 ppm) is seen at C8 carbon and the same was theoretically computed at 173.3 ppm. The ^{1}H atom is the smallest of all atoms and hence most part of the atom is confined on fringe of molecules; along these lines their chemical shifts would be more vulnerable to intermolecular interactions in the fluid arrangements when contrasted with that of other heavier atoms. For ^{1}H chemical shifts, the most extreme deviation from experimental value is calculated at H18 (12.11 ppm) since the hydrogen bonds formation in between H18 and O29 which prompts a significant down-field shift of the isotropic chemical shifts and this values is also calculated at 7.19 ppm. The experimental chemical shift value of H28 (OH) is 8.98 ppm, which is higher than other H (OH). The hydrogen-bond formation has been made in between hydroxyl protons and the carbonyl group and hence the electron density shift from the OH to the carbonyl group results in an increased magnetic shielding for the hydroxyl proton. We have also calculated a similar inducement at 8.98 ppm besides the other computed ^{1}H and ^{13}C chemical shifts values, which are in concurrence with the experimental values.

Frontier molecular orbital analysis: The highest occupied molecular orbital (HOMO) and the lowest unoccupied molecular orbital (LUMO) represents its ability to donate and accept electron, respectively. From the molecular orbital theory, the π-π* transition state is calculated because of the interaction between the HOMO and LUMO [54]. In general, the HOMO and LUMO energy gap is related with polarizable, chemical reactivity and kinetic stability. The molecule, which have low

frontier orbital gap (HOMO-LUMO gap) is more polarizable, highly chemically reactive and has low kinetic stability, which also termed as soft molecule [55]. The HOMO-LUMO energy gap and their corresponding density of state (DOS) of kaempferide as shown in Fig. 4. The HOMO is primarily localized over the chromone and phenyl ring and the LUMO is confined over all to the part of the molecule. The HOMO and LUMO energy is -6.0138 eV and -1.9048 eV, respectively and the HOMO-LUMO energy gap is 4.1090 eV.

UV-visible and electronic properties: The UV-visible absorption spectrum of the solvated KFD molecule in methanol was investigated theoretically by means of TD-DFT/B3LYP/6-31G(d,p) method. The calculated results involving the vertical excitation energies, oscillator strength (f) and wavelength are carried out and have been used to determine the low-lying excited states of KFD. Table-4 shows the electronic absorption wave lengths and oscillator strengths calculated by TDDFT/6-31G (d,p) method in methanol. For a lack of experimental information we cannot compare the $\pi \rightarrow \pi^*$ transitions calculated in the present work. However, according to Frank-Condon principle, the maximum absorption peak correspond in UV-visible spectrum to vertical excitation predicts one intense electronic transition at 350.02 nm with an oscillator strength f = 0.5234. This strong absorption peak is caused by the $\pi \rightarrow \pi^*$ transitions and the other weak bands due to n-π transition are calculated at 323.79 and 309.45 nm, respectively. The energy gap of HOMO-LUMO explains the charge transfer interaction within the molecule and the frontier orbital gap of KFD is found to be 4.1090 eV. The calculated absorption energy at TD-DFT method using 6-311++G (d,p) basis set is 3.5422 eV. It has been conclude that the lowest singlet excited state of the KFD molecule is mainly derived from the HOMO→LUMO ($\pi \rightarrow \pi^*$) electron transition. Also, The $\pi \rightarrow \pi^*$ transition energy was computed to be 350.02 nm is indeed reproduced the available experimental results of the quercetin [56] and keampferol [57] in methanol solution.

Molecular electrostatic potential energy surface: The electrostatic potential [V(r)] of molecular system is expressed in terms of the electronic charge density and is rapidly becoming a consistently used tool in the investigation of molecular reactivity in both academic and industrial research [58,59]. Fig. 5 shows molecular electrostatic potential surface and contour map of the KFD computed at B3LYP/6311G++(d,p). As can be seen from Fig. 5, the colour code of the MEP map was in the range between -6.019 e^{-2} (deep red) and +6.019 e^{-2} (deep blue). The positive (blue) and negative (red) region exhibits the possible nucleophilic and electrophilic sites, respectively and the V(r) values were acquired on molecular surface characterized by electron density with 0.001 electron/bohr^3. The negative regions in the molecules were found around the

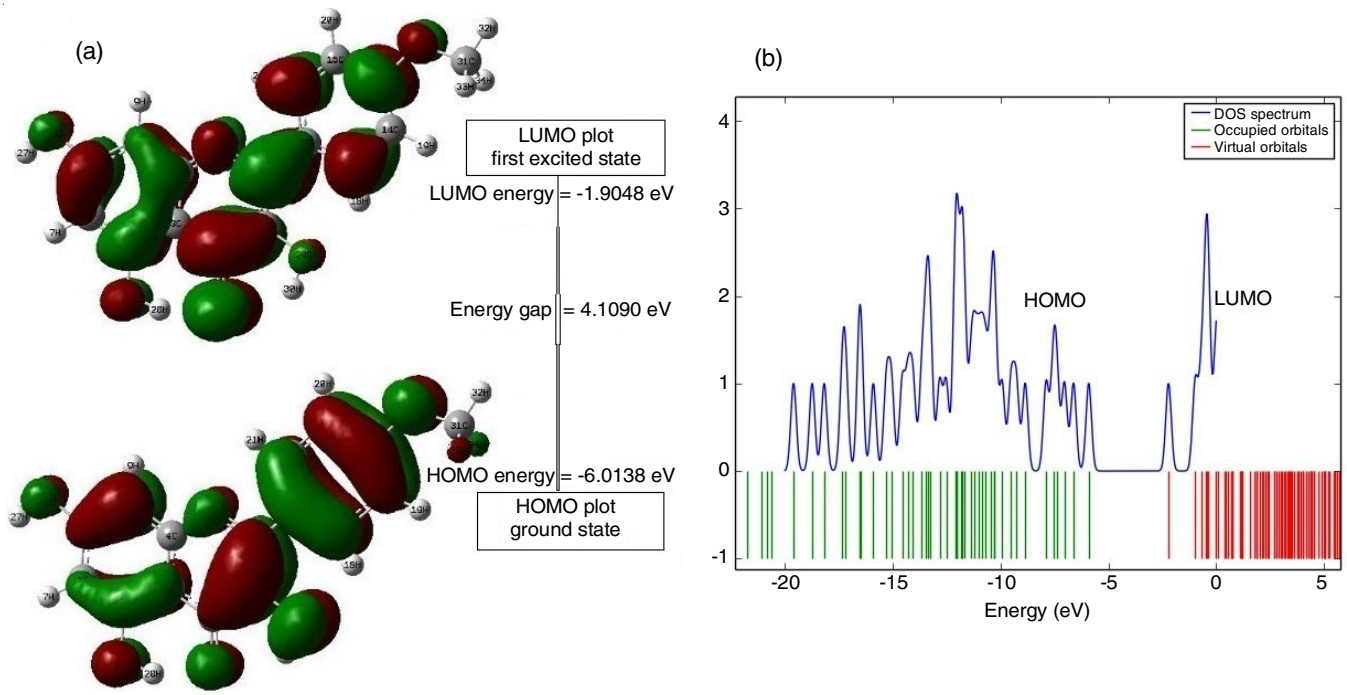

Fig. 4. (a) HOMO-LUMO energy gap (b) corresponding density of state (DOS) of kaempferide

TABLE-4
THEORETICALLY CALCULATED ABSORPTION WAVELENGTH
OSCILLATOR STRENGTH AND EXCITATION ENERGY OF KAEMPFERIDE

Experimental λ_{max} (nm) in methanol				TD-DFT/6-311++G(d,p) level		
Quercetin [Ref. 32]		Kaempferol [Ref. 33]		λ_{max} (nm)	Osc. strength	E (eV)
Band I	Band II	Band I	Band II			
372	256	366	267	350.02	0.5234	3.5422
	254		266	323.79	0.1079	3.8292
	230		264	309.45	0.1525	4.0066

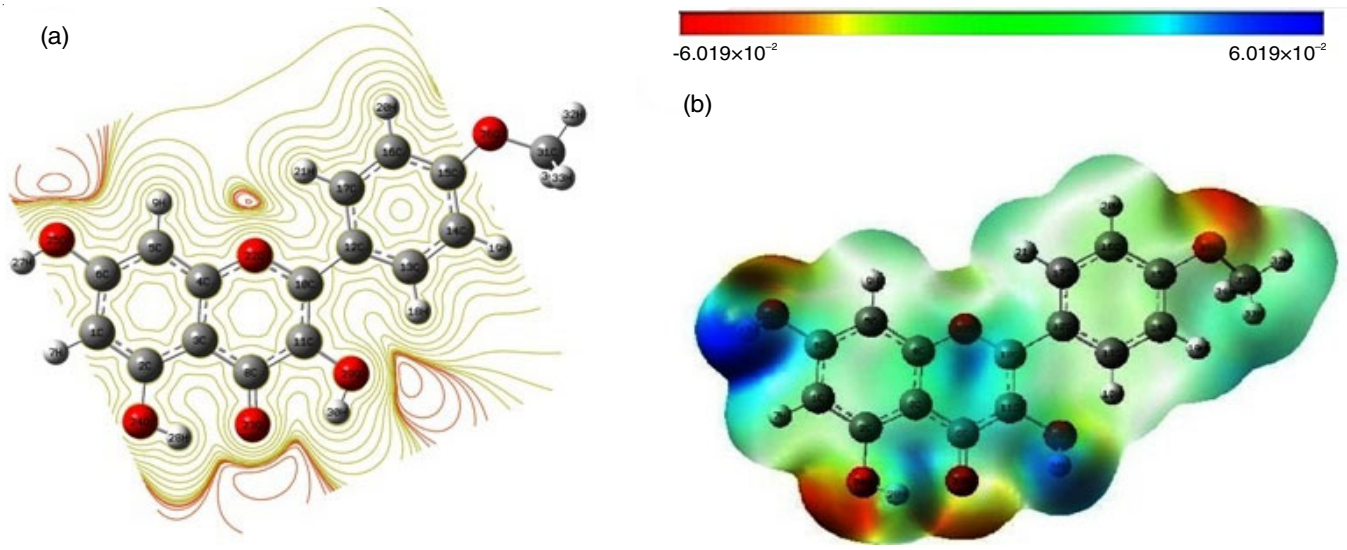

Fig. 5. (a) Contour map (b) total electron density isosurface mapped with molecular electrostatic potential of kaempferide

carbonyl O23, O22, O26 and hydroxyl O24, O25 and O29 atoms and hence, it is expected that it will be favoured for electrophilic attack or strongest pushing of electron. It is fascinating to note that the blue region is a biggest positive locale, which is mostly confined over the hydrogen atoms like H27, H28, H30 and exhibits nucleophilic attack or strongest pulling of electron.

Molecular docking study: Molecular docking is a well established computational tool which predicts the interaction energy between small molecule and a protein at the atomic level, commonly applied in drug discovery. Also it enables us to characterize the behaviour of small molecules in the binding site of target proteins and elucidate fundamental biochemical processes [60]. Molecular docking investigation is performed on the optimized molecular structure of the KFD using Autodock 4.2 with mgltools 1.5.6. [41]. The crystal structure of Human Cytochrome P450 1A1 in complex with α-naphthoflavone (PDB ID: 4I8V), Human Microsomal P450 1A2 in complex with alphanaphthoflavone (PDB ID: 2HI4), Crystal Structure of CYP450 2C9 with flurbiprofen bound (PDB ID: IR9O), crystal structure of human cytochrome CYP450 3A4 bound to an inhibitor ritonavir (PDB ID: ITQN), crystal structure of human cytochrome P450 2D6 with prinomastat bound (PDB ID:3QM4) and CYP2C8dH complexed with montelukast (PDB ID: 2NNI) were downloaded from protein data bank [61]. All the torsion bond of the ligand (KFD) were set free to perform flexible docking while the macromolecule (cytochrome P450) were kept rigid. The hydrogen bond interactions of the KFD against CYPs (1A1, 1A2, 3A4, 2C8, 2C9 and 2D6) were as shown in Fig. 6. The predicted docking energies, inhibition constant and hydrogen bond interaction are listed in the Table-5. The inhibition activity of CYPs by various flavonoid has been reported in a few investigations [62,63]. In line with previous literature, this present molecular docking study also demonstrated that the KFD effectively interact with CYPs proteins and these adaptation were balanced out by a hydrogen bond interaction either with backbone or side chain of the residues including Arg93, Gly453, Arg464, Glu445 (PDB:4I8V), Asn247, Gln251, Lys254 (PDB:2HI4), Thr305, Gln356, Thr302, Pro427, Thr302 (PDB:1R9O),Val104, Tyr56, Arg63, Phe112, Asp50 (PDB:3QM4), Thr310, Pro434 (PDB:1TQN) and Thr302, Thr305, Leu361, Val362, Cys435, Gln356, Thr302, Ala297 (PDB:2NNI). It was evident from the molecular electrostatic potential (Fig. 5) map that the maximum positive potential was concentrated on the H27, H28 and H30 atoms of the hydroxyl group, which is a suitable site for nucleophilic reactivity. From Fig. 6, it was confirmed that the H27, H28 and H30 atoms of hydroxyl group acted as a donor atom and involves hydrogen bond interaction with the residues Pro434, Ala297, Asp50, Tyr244, Thr302, Thr305 and Glu445. Similarly, From Fig. 5, the maximum negative region were found around the carbonyl O23, O28, hydroxyl O24, O25 and methoxyl O26 atoms were expected that it was a preferred site for electrophilic attack. It was evident that from Fig. 6 that O22 and O23 atoms of carbonyl group indicated hydrogen bond interaction with Lys254, Arg63 and Arg93, Thr302, respectively whereas O24 atom of hydroxyl group showed hydrogen bond interaction with Thr302 and Gln356. Also, the O25 atom of the hydroxyl group showed hydrogen bond interaction with Gly453, Asn247 and Cys435 at the same time as the O26 atom of the methoxyl group showed hydrogen bond interaction with Arg464, Leu361, Val362 and Val104. From the nucleophilic and electrophilic sites, the intermolecular interaction of the title compound with the proteins can be understood based on the information provided by molecular docking study. The inhibition mechanism of the investigated compound is also supports the inhibition of similar derivatives with CYP450 enzymes, those already reported by different authors [62,63]. CYP2C9 shares over 80% amino acids sequence identity with CYP2C8 [64] and expressed in the abnormal states in the human liver [65]. Our outcomes additionally affirm that the kaempferide demonstrates a better binding affinity with the residues of CYP2C8 (PDB: 2NNI) and CYP2C9 (PDB: 1R9O) and the minimum binding energy is -9.43 kcal/mol and -8.53 kcal/mol, respectively. The CYP450 2C8 enzyme metabolizes various anticancer drugs [66] and it is worth underlining that these protein inhibition scores strengthen the possibility of anticancer activity and may have an imperative part in clinical trials.

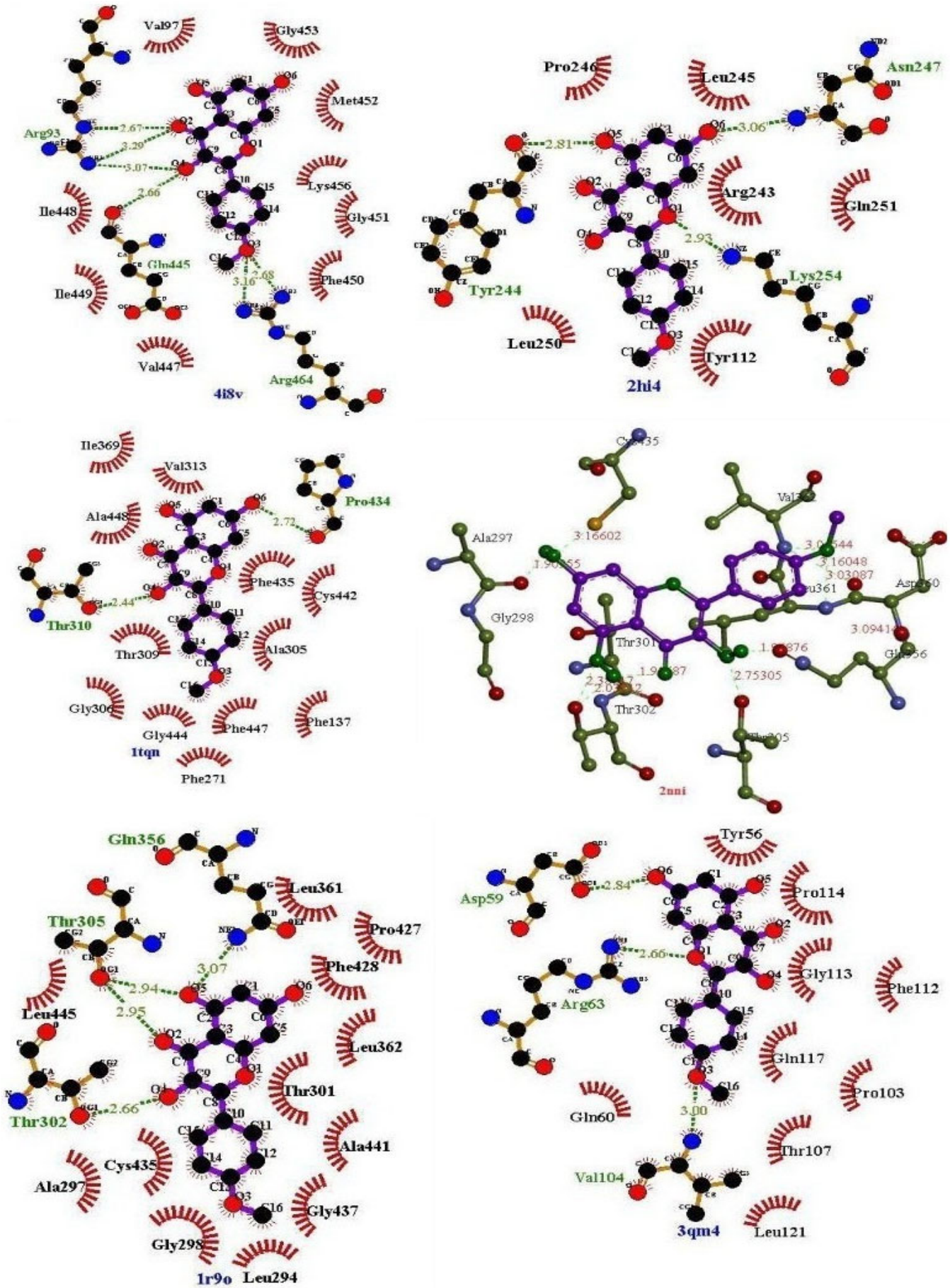

Fig. 6. Amino acid interactions of CYPs with the stick model of kaempferide. Hydrogen bond interaction either with backbone or side chain of the residues is indicated by dotted green lines

TABLE-5
PREDICTED BINDING ENERGIES, INHIBITION CONSTANT, INTERACTION OF AMINO ACIDS AND H-BOND ANALYSIS OF DIFFERENT TARGET PROTEINS WITH KFD

Name of the target protein	Binding energy (kcal/mol)	Estimated inhibition constant (μM)	Binding site interaction	Donor	Acceptor	H-Bond distance (Å)
CYP1A1 PDB:4I8V	-7.49	3.25	ARG93-Ligand	NE	O	2.665
			ARG93-Ligand	NH_2	O	3.070
			ARG464-Ligand	NH1	O	3.161
			ARG464-Ligand	NH2	O	2.682
			GLY453-Ligand	N	O	2.852
			Ligand-GLU445	H	O	2.165
CYP1A2 PDB:2HI4	-6.62	14.12	ASN247-Ligand	N	O	3.064
			GLN251-Ligand	NE2	O	3.101
			LYS254-Ligand	NZ	O	2.931
			Ligand-TYR214	H	O	2.145
CYP3A4 PDB:1TQN	-8.34	0.769	THR310-Ligand	OG1	O	2.436
			Ligand-THR310	H	OG1	2.184
			Ligand-PRO434	H	O	1.795
CYP2C8 PDB:2NNI	-9.43	0.121	THR302-Ligand	OG1	O	2.386
			THR305-Ligand	OG1	O	2.753
			LEU361-Ligand	N	O	3.030
			VAL362-Ligand	N	O	3.065
			CYS435-Ligand	SG	O	3.166
			Ligand-GLN356	H	OE1	1.968
			Ligand-THR302	H	OG1	2.038
			Ligand-ALA297	H	O	1.909
CYP2C9 PDB:1R9O	-8.53	0.555	THR302-Ligand	OG1	O	2.664
			THR305-Ligand	OG1	O	2.951
			GLN356-Ligand	OG1	O	2.939
			Ligand-THR302	H	OG1	1.780
			Ligand-PRO427	H	O	1.742
CYP2D6 PDB:3QM4	-7.08	6.51	VAL104-Ligand	N	O	2.997
			TYR56-Ligand	OH	O	2.910
			ARG63-Ligand	NH1	O	2.660
			Ligand-PHE112	H	O	2.197
			Ligand-ASP50	H	OD1	2.082

Conclusion

The molecular structural parameters, wavenumbers and the corresponding vibrational assignments of KFD were studied by both DFT and experimental method. The consistency between the calculated and experimental FTIR and FT-Raman data demonstrates that the DFT method can generate reliable geometry and related properties of the KFD. The ^{1}H and ^{13}C NMR magnetic isotropic chemical shifts of the KFD were computed by GIAO/B3LYP/6-31G (d) method and compared with experimental one. The HOMO-LUMO energy gab explains the charge transfer takes place in the molecule. The results of the TED calculation are also useful for understanding the maximum absorption wavelength, excitation energy and oscillator strength involved in the compound. The most reactive part in the molecule is identified by MEP analysis and it can be understood based on the information provided by molecular docking study. The results of molecular docking study shows that the title molecule can easily dock with CYPs 1A1, 1A2, 3A4, 1B1, 2C8, 2C9 and 2D6 proteins by influencing a hydrogen bond interaction. Remarkably, the KFD shows better binding mechanism with the residues of the CYP2C8 and CYP2C9 with minimum binding energy -9.43 kcal/mol and -8.53 kcal/mol, respectively. As a result, these outcomes strengthen the possibility of anticancer activity and may have significant counteractive action for various diseases.

ACKNOWLEDGEMENTS

The authors are thankful to Sophisticated Analytical Instrumentation Facility (SAIF), IIT Madras for FT-Raman studies.

REFERENCES

1. G.R. Beecher, Overview of Dietary Flavonoids: Nomenclature, Occurrence and Intake, *J. Nutr*., **133**, 3248S (2003); https://doi.org/10.1093/jn/133.10.3248S
2. J.A. Ross and C.M. Kasum, Dietary Flavonoids: Bioavailability, Metabolic Effects and Safety, *Annu. Rev. Nutr*., **22,** 19 (2002); https://doi.org/10.1146/annurev.nutr.22.111401.144957
3. M. Asif and E. Khodadadi, Medicinal Uses and Chemistry of Flavonoid Contents of Some Common Edible Tropical Plants, *J. Paramed. Sci*., **4**, 119 (2013); https://doi.org/10.22037/JPS.V4I3.4648
4. D. Liu, W. Qu and J.Y. Liang, Flavonoids and Other Constituents from *Alpinia sichuanensis* Z.Y. Zhu, *Biochem. System. Ecol*., **46**, 127 (2013); https://doi.org/10.1016/j.bse.2012.09.022
5. V. Martineti, I. Tognarini, C. Azzari, S.C. Sala, F. Clematis, M. Dolci, V. Lanzotti, F. Tonelli, M.L. Brandi and P. Curir, Inhibition of *in vitro* Growth and Arrest in the G0/G1 Phase of HCT8 Line Human Colon Cancer Cells by Kaempferide Triglycoside from *Dianthus caryophyllus*, *Phytother Res*., **24**, 1302 (2010); https://doi.org/10.1002/ptr.3105
6. H. Gao, B. Liu, F. Liu and Y.S. Chen, Anti-Proliferative Effect of Camellianin A in Adinandra nitida Leaves and Its Apoptotic Induction in Human Hep G2 and MCF-7 Cells, *Molecules* **15**, 3878 (2010); https://doi.org/10.3390/molecules15063878

7. A.K. Calgarotto, S. Miotto, K.M. Honorio, A.B.F. Da Silva, S. Marangoni, J.L. Silva, M. Comar Jr., K.M.T. Oliveira and S.L. da Silva, A Multivariate Study on Flavonoid Compounds Scavenging the Peroxynitrite Free Radical, *J. Mol. Struct. Theochem.*, **808**, 25 (2007); https://doi.org/10.1016/j.theochem.2006.12.031
8. L.R. Nath, J.N. Gorantla, S.M. Joseph, J. Antony, S. Thankachan, D.B. Menon, S. Sankar, R.S. Lankalapalli and R.J. Anto, Kaempferide, The Most Active Among the Four Flavonoids Isolated and Characterized from *Chromolaena odorata*, Induces Apoptosis in Cervical Cancer Cells While Being Pharmacologically Safe, *RSC Adv*., **5**, 100912 (2015); https://doi.org/10.1039/C5RA19199H
9. H. Tani, K. Hasumi, T. Tatefuji, K. Hashimoto, H. Koshino and S. Takahashi, Inhibitory Activity of Brazilian Green Propolis Components and their Derivatives on the Release of cys-Leukotrienes, *Bioorg. Med. Chem.*, **18**, 151 (2010); https://doi.org/10.1016/j.bmc.2009.11.007
10. A.H. Banskota, Y. Tezuka, J.K. Prasain, K. Matsushige, I. Saiki and S. Kadota, Chemical Constituents of Brazilian Propolis and Their Cytotoxic Activities, *J. Nat. Prod*., **61**, 896 (1998); https://doi.org/10.1021/np980028c
11. E. Srinivasan and R. Rajasekaran, Comparative Binding of Kaempferol and Kaempferide in Inhibiting the Aggregate Formation of Mutant (G85R) SOD1 Protein in Familial Amyotrophic Lateral Sclerosis: A Quantum Chemical and Molecular Mechanics Study, *BioFactors*, **44**, 431(2018); https://doi.org/10.1002/biof.1441
12. D. Wang, X. Zhang, D. Li, W. Hao, F. Meng, B. Wang, J. Han and Q. Zheng, Kaempferide Protects against Myocardial Ischemia/Reperfusion Injury through Activation of the PI3K/Akt/GSK-3β Pathway, *Mediators of Inflamm.*, **2017**, 5278218 (2017); https://doi.org/10.1155/2017/5278218
13. V.-S. Nguyen, L. Shi, F.-Q. Luan and Q.-A. Wang, Synthesis of Kaempferide Mannich Base Derivatives and their Antiproliferative Activity on Three Human Cancer Cell Lines, *Acta Biochim. Polon*., **62**, 547 (2015); https://doi.org/10.18388/abp.2015_992
14. Z. Ji, B. Wang, K. Yan, L. Dong, G. Meng and L. Shi, A Linear Programming Computational Framework Integrates Phosphor-Proteomics and Prior Knowledge to Predict Drug Efficacy, *BMC Syst. Biol*., **11**, 103 (2017); https://doi.org/10.1186/s12918-017-0501-6
15. S. Kumkarnjana, R. Suttisri, U. Nimmannit, A. Sucontphunt, M. Khongkow, T. Koobkokkruad and N. Vardhanabhuti, Flavonoids Kaempferide and 4,2′-Dihydroxy-4′,5′,6′-trimethoxychalcone Inhibit Mitotic Clonal Expansion and Induce Apoptosis During the Early Phase of Adipogenesis in 3T3-L1 Cells, *J. Integr. Med*., **17**, 288 (2019); https://doi.org/10.1016/j.joim.2019.04.004
16. Y.S. Loh, G. Li, K. Fan, I. Ahmed, B. Roufogalis and D. Sze, Kaempferide Targets Side Population, the Putative Cancer Stem Cell, in Myeloma and Induced Apoptosis in Dose-Dependant Manner, *Blood*, **116**, 5029 (2010); https://doi.org/10.1182/blood.V116.21.5029.5029
17. J.P. Abraham, I.H. Joe, V. George, O.F. Nielsen and V.S. Jayakumar, Vibrational Spectroscopic Studies on the Natural Product, Columbianadin, *Spectrochim. Acta A Mol. Biomol. Spectrosc*., **59**, 193 (2003); https://doi.org/10.1016/S1386-1425(02)00148-8
18. Y. Erdogdu, O. Unsalan and M.T. Gulluoglu, Vibrational Analysis of Flavone, *Turk. J. Phys*., **33**, 249 (2009).
19. D. Milenkovic, J.M.D. Markovic, D. Dimic, S. Jeremic, D. Amic, M.S. Pirkovic, Z.S. Markovic, Structural Characterization of Kaempferol: A Spectroscopic and Computational Study, *Maced. J. Chem. Chem. Eng*., **38**, 49 (2019); https://doi.org/10.20450/mjcce.2019.1333
20. A.M. Mendoza-Wilson and D. Glossman-Mitnik, CHIH-DFT Determination of the Molecular Structure, Infrared and Ultraviolet Spectra of the Flavonoid Quercetin, *J. Mol. Struct. (Theochem.)*, **681**, 71 (2004); https://doi.org/10.1016/j.theochem.2004.04.054
21. G. Mariappan, N. Sundaraganesan and S. Manoharan, The Spectroscopic Properties of Anticancer Drug Apigenin Investigated by using DFT Calculations, FT-IR, FT-Raman and NMR Analysis, *Spectrochim. Acta A Mol. Biomol. Spectrosc.*, **95**, 86 (2012); https://doi.org/10.1016/j.saa.2012.04.089
22. N. Sundaraganesan, G. Mariappan and S. Manoharan, Molecular Structure and Vibrational Spectroscopic Studies of Chrysin using HF and Density Functional Theory, *Spectrochim. Acta A Mol. Biomol. Spectrosc*., **87**, 67 (2011); https://doi.org/10.1016/j.saa.2011.11.011
23. J.P. Cornard, L. Vrielynck, J.C. Merlin and J.C. Wallet, Structural and Vibrational Study of 3-Hydroxyflavone and 3-Methoxyflavone, *Spectrochim. Acta A Mol. Biomol. Spectrosc*., **51**, 913 (1995); https://doi.org/10.1016/0584-8539(94)01425-G
24. F.P. Guengerich, Z.L. Wu and C.J. Bartleson, Function of Human Cytochrome P450s: Characterization of the Orphans, *Biochem. Biophys. Res. Commun*., **338**, 465 (2005); https://doi.org/10.1016/j.bbrc.2005.08.079
25. F.P. Guengerich, Cytochrome P450s and Other Enzymes in Drug Metabolism and Toxicity, *AAPS J*., **8**, E101(2006); https://doi.org/10.1208/aapsj080112
26. V.M. Breinholt, E.A. Offord, C. Brouwer, S.E. Nielsen, K. Brøsend and T. Friedberge, *in vitro* Investigation of Cytochrome P450-Mediated Metabolism of Dietary Flavonoids, *Food Chem Toxicol*., **40**, 609 (2002); https://doi.org/10.1016/S0278-6915(01)00125-9
27. T. Shimada, K. Tanaka, S. Takenaka, N. Murayama, M.V. Martin, M.K. Foroozesh, H. Yamazaki, F.P. Guengerich and M. Komori, Structure-Function Relationships of Inhibition of Human Cytochromes P450 1A1, 1A2, 1B1, 2C9, and 3A4 by 33 Flavonoid Derivatives, *Chem. Res. Toxicol*., **23**, 1921 (2010); https://doi.org/10.1021/tx100286d
28. M. Bojic, M. Kond•a, H. Rimac, G. Benkovic and •. Maleš, The Effect of Flavonoid Aglycones on the CYP1A2, CYP2A6, CYP2C8 and CYP2D6 Enzymes Activity, *Molecules*, **24**, 3174. (2019); https://doi.org/10.3390/molecules24173174
29. J. Sridhar, J. Ellis, P. Dupart, J. Liu, C.L. Stevens and M. Foroozesh, Development of Flavone Propargyl Ethers as Potent and Selective Inhibitors of Cytochrome P450 Enzymes 1A1 and 1A2, *Drug Metab. Lett.*, **6**, 275 (2012); https://doi.org/10.2174/1872312811206040007
30. J. Sridhar, N. Goyal, J. Liu and M. Foroozesh, Review of Ligand Specificity Factors for CYP1A Subfamily Enzymes from Molecular Modeling Studies Reported to-Date, *Molecules*, **22**, 1143 (2017); https://doi.org/10.3390/molecules22071143
31. F. Iori, R. da Fonseca, M.J. Ramos and M.C. Menziani, Theoretical Quantitative Structure-Activity Relationships of Flavone Ligands Interacting with Cytochrome P450 1A1 and 1A2 Isozymes, *Bioorg. Med. Chem*., **13**, 4366 (2005); https://doi.org/10.1016/j.bmc.2005.04.066
32. R. Santes-Palacios, A. Romo-Mancillas, R. Camacho-Carranza and J.J. Espinosa-Aguirre, Inhibition of Human and Rat CYP1A1 Enzyme by Grapefruit Juice Compounds, *Toxicol. Lett*., **258**, 267 (2016); https://doi.org/10.1016/j.toxlet.2016.07.023
33. A. G. Indu, Punnagai Munusami, C. S. Vasavi and G. Divya, Molecular Docking Studies on Flavonoid Compounds: An Insight into Aromatase Inhibitors, *Int. J. Pharm. Pharm. Sci*., **6**, 141 (2014)
34. M.C. Sousa, R. C. Braga, B.A.S. Cintra, V. de Oliveira and C. H. Andrade, *in silico* Metabolism Studies of Dietary Flavonoids by CYP1A2 and CYP2C9, *Food Res. Int*., **50**, 102 (2013); https://doi.org/10.1016/j.foodres.2012.09.027
35. H. Takemura, T. Itoh, K. Yamamoto, H. Sakakibara and K. Shimoi, Selective Inhibition of Methoxyflavonoids on Human CYP1B1 Activity, *Bioorg. Med. Chem*., **18**, 6310 (2010); https://doi.org/10.1016/j.bmc.2010.07.020
36. V. P. Androutsopoulos, A. Papakyriakou, D. Vourloumis and D. A. Spandido, Comparative CYP1A1 and CYP1B1 Substrate and Inhibitor Profile of Dietary Flavonoids, *Bioorg. Med. Chem*., **19**, 2842 (2011); https://doi.org/10.1016/j.bmc.2011.03.042
37. L. Quintieri, S. Bortolozzo, S. Stragliotto, S. Moro, M. Pavanetto, A. Nassi, P. Palatini and M. Floreani, Flavonoids Diosmetin and Hesperetin are Potent Inhibitors of Cytochrome P450 2C9-Mediated Drug Metabolism i*n vitro*, *Drug Metab. Pharmacokin*., **25**, 466 (2010); https://doi.org/10.2133/dmpk.DMPK-10-RG-044
38. Pius Fasinu, Y.E. Choonara, R.A. Khan, L.C. Du Toit, P. Kumar, V.M.K. Ndesendo and V. Pillay, Flavonoids and Polymer Derivatives as CYP3A4 Inhibitors for Improved Oral Drug Bioavailability, *J Pharm Sci*., **102**, 541(2013); https://doi.org/10.1002/jps.23382

39. D.Z. Tu, H.Y. MA, Y.Q. Wang and X.-H Zhao, W.Z. Guo G.B. Ge and L. Yang, Inhibitory Effect of Flavonoids from *Scutellariae radix* on Human Cytochrome P450 1A, *China J. Chinese Mater. Med*., **44**, 566 (2019); https://doi.org/10.19540/j.cnki.cjcmm.20181128.005-en
40. M.J. Frisch, G.W. Trucks, H.B. Schlegel, G.E. Scuseria, M.A. Robb, J.R. Cheeseman, G. Scalmani, V. Barone, G.A. Petersson, H. Nakatsuji, X. Li, M. Caricato, A. Marenich, J. Bloino, B. G. Janesko, R. Gomperts, B. Mennucci, H.P. Hratchian, J.V. Ortiz, A.F. Izmaylov, J.L. Sonnenberg, D. Williams-Young, F. Ding, F. Lipparini, F. Egidi, J. Goings, B. Peng, A. Petrone, T. Henderson, D. Ranasinghe, V.G. Zakrzewski, J. Gao, N. Rega, G. Zheng, W. Liang, M. Hada, M. Ehara, K. Toyota, R. Fukuda, J. Hasegawa, M. Ishida, T. Nakajima, Y. Honda, O. Kitao, H. Nakai, T. Vreven, K. Throssell, J.A. Montgomery, Jr., J.E. Peralta, F. Ogliaro, M. Bearpark, J.J. Heyd, E. Brothers, K.N. Kudin, V.N. Staroverov, T. Keith, R. Kobayashi, J. Normand, K. Raghavachari, A. Rendell, J.C. Burant, S.S. Iyengar, J. Tomasi, M. Cossi, J.M. Millam, M. Klene, C. Adamo, R. Cammi, J.W. Ochterski, R.L. Martin, K. Morokuma, O. Farkas, J.B. Foresman and D.J. Fox, Gaussian 09, Revision A.02 Gaussian Inc Wallingford CT (2016).
41. R. Huey and G.M. Morris, Using AutoDock 4 with AutoDocktools: A Tutorial, The Scripps Research Institute, Molecular Graphics Laboratory, La Jolla, CA, USA (2008).
42. Z.Y. Chen, P.T. Chan, K.Y. Ho, K.P. Fung and J. Wang, Antioxidant Activity of Natural Flavonoids is Governed by Number and Location of their Aromatic Hydroxyl Groups, *Chem. Phys. Lipids*, **79**, 157 (1996); https://doi.org/10.1016/0009-3084(96)02523-6
43. D. Amic, D. Davidovic-Amic, D. Beslo, V. Rastija, B. Lucic and N. Trinajstic, SAR and QSAR of the Antioxidant Activity of Flavonoids, *Curr. Med. Chem*., **14**, 827 (2007); https://doi.org/10.2174/092986707780090954
44. I.M. Ross, F.L. Rickles and A. W. Halpin, The Crystal and Molecular Structure of Quercetin: A Biologically Active and Naturally Occurring Flavonoid, *Bioorg. Chem*., **14**, 55 (1986); https://doi.org/10.1016/0045-2068(86)90018-0
45. M.L. Martinez and S.L. Studer and P.T. Chou, Direct Evidence of the Excited-State Intramolecular Proton Transfer in 5-Hydroxyflavone, *J. Am. Chem. Soc*., **113**, 5881 (1991); https://doi.org/10.1021/ja00015a063
46. E. Falkovskaia, P.K. Sengupta and M. Kasha, Photophysical Induction of Dual Fluorescence of Quercetin and Related Hydroxyflavones Upon Intermolecular H-Bonding to Solvent Matrix, *Chem. Phys Lett*., **297**, 109 (1998); https://doi.org/10.1016/S0009-2614(98)01112-9
47. H.B. Liu, Y. Daun, S.C. Shin, H.R. Park, J.K. Park and K.-M. Bark, Spectroscopic Properties of Quercetin Derivatives, Quercetin-3-O-rhamnoside and Quercetin-3-O-rutinoside, in Hydro-organic Mixed Solvents, *Photochem. Photobiol*., **85**, 934 (2009); https://doi.org/10.1111/j.1751-1097.2009.00550.x
48. G.Z. Jin, Y. Yamagata and K. Tomita, Structure of Quercetin Dihydrate, *Acta Cryst.,* **C46**, 310 (1990); https://doi.org/10.1107/S0108270189006682
49. H. Angamuthu and M. Ramachandrane, Investigations on the Structural, Vibrational, Computational and Molecular Docking Studies on the Potential Antidiabetic Chemical Agent Diosmetin, *J. Mol. Recognit*., **33**, e2819 (2020); https://doi.org/10.1002/jmr.2819
50. N.B. Neilson and A.J. Holder, GAUSS VIEW 5.0, User's Reference, Gaussian Inc., Pittsburgh, CT (2009).
51. M.H. Jamroz, Vibrational Energy Distribution Analysis: VEDA 4 Computer Program, Poland, p. 174 (2004).
52. H.O. Kalinowski, S. Berger and S. Brawn, Carbon-13 NMR Spectroscopy, John Wiley & Sons, Chichester (1988).
53. K. Pihlaja, E. Kleinpeter, Carbon13 Chemical Shifts in Structural and Sterochemical Analysis, VCH Publishers, Deereld Beach, FL (1994).
54. K. Fukui, Theory of Orientation and Stereo Selection, Springer-Verlag, Berlin (1975).
55. I. Fleming, Frontier Orbitals and Organic Chemical Reactions, John Wiley & Sons: New York (1976).
56. J.P. Cornard, L. Dangleterre and C. Lapouge, Computational and Spectroscopic Characterization of the Molecular and Electronic Structure of the Pb(II)-Quercetin Complex, *J. Phys. Chem. A,* **109**, 10044 (2005); https://doi.org/10.1021/jp053506i
57. D.R. Telange, A.T. Patil, A. Tatode and B. Bhoyar, Development and Validation of UV Spectrophotometric Method for the Estimation of Kaempferol in Kaempferol: Hydrogenated Soy PhosphatidylCholine (HSPC) Complex, *Pharm. Methods*, **5**, 34 (2014); https://doi.org/10.5530/phm.2014.1.6
58. E. Scrocco and J. Tomasi, Electronic Molecular Structure, Reactivity and Intermolecular Forces: An Euristic Interpretation by Means of Electrostatic Molecular Potentials, *Adv. Quant. Chem.,* **11**, 115 (1978); https://doi.org/10.1016/S0065-3276(08)60236-1
59. F.J. Luque, J.M. Lopez and M. Orozco, Perspective on Electrostatic Interactions of a Solute with a Continuum. A Direct Utilization of *ab initio* Molecular Potentials for the Prevision of Solvent Effects, *Theor Chem Acc*., **103**, 343 (2000); https://doi.org/10.1007/s002149900013
60. B.J. McConkey, V. Sobolev and M. Edelman, The Performance of Current Methods in Ligand-Protein Docking, *Curr. Sci*., **83**, 845 (2002); https://doi.org/10.2307/24107087
61. http://www.rcsb.org/pdb
62. L. Quintieri, P. Palatini, S. Moro and M. Floreani, Inhibition of Cytochrome P450 2C8-mediated Drug Metabolism by the Flavonoid Diosmetin, *Drug Metab. Pharmacokin*., 26, 559 (2011); https://doi.org/10.2133/dmpk.DMPK-11-RG-048
63. M. Ridderstrom, I. Zamora, O. Fjellström and T.B. Andersson, Analysis of Selective Regions in the Active Sites of Human Cytochromes P450, 2C8, 2C9, 2C18, and 2C19 Homology Models Using GRID/CPCA, *J. Med. Chem.,* **44**, 4072 (2001); https://doi.org/10.1021/jm0109107
64. S. Rendic and F.J. Di Carlo, Human Cytochrome P450 Enzymes: A Status Report Summarizing their Reactions, Substrates, Inducers and Inhibitors, *Drug Metab. Rev*., **29**, 413 (1997); https://doi.org/10.3109/03602539709037591
65. R.A. Totah and A.E. Rettie, Cytochrome P450 2C8: Substrates, Inhibitors, Pharmacogenetics and Clinical Relevance, *Clin. Pharmacol. Ther*., **77**, 341 (2005); https://doi.org/10.1016/j.clpt.2004.12.267